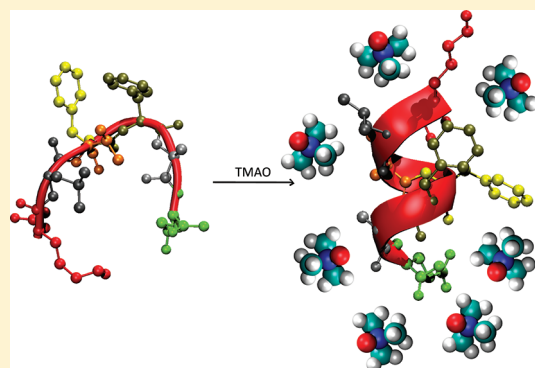


Entropic Stabilization of Proteins by TMAO

Samuel S. Cho,^{†,‡} Govardhan Reddy,[†] John E. Straub,[§] and D. Thirumalai^{*,†}[†]Department of Chemistry and Biochemistry and Biophysics Program, Institute for Physical Science and Technology, University of Maryland, College Park, Maryland 20742, United States[§]Department of Chemistry, Boston University, Boston, Massachusetts 02215, United States Supporting Information

ABSTRACT: The osmolyte trimethylamine *N*-oxide (TMAO) accumulates in the cell in response to osmotic stress and increases the thermodynamic stability of folded proteins. To understand the mechanism of TMAO induced stabilization of folded protein states, we systematically investigated the action of TMAO on several model dipeptides (leucine, L₂, serine, S₂, glutamine, Q₂, lysine, K₂, and glycine, G₂) in order to elucidate the effect of residue-specific TMAO interactions on small fragments of solvent-exposed conformations of the denatured states of proteins. We find that TMAO preferentially hydrogen bonds with the exposed dipeptide backbone but generally not with nonpolar or polar side chains. However, interactions with the positively charged Lys are substantially greater than with the backbone. The dipeptide G₂ is a useful model of the pure amide backbone; interacts with TMAO by forming a hydrogen bond between the amide nitrogen and the oxygen in TMAO. In contrast, TMAO is depleted from the protein backbone in the hexapeptide G₆, which shows that the length of the polypeptide chain is relevant in aqueous TMAO solutions. These simulations lead to the hypothesis that TMAO-induced stabilization of proteins and peptides is a consequence of depletion of the solute from the protein surface provided intramolecular interactions are more favorable than those between TMAO and the backbone. To test our hypothesis, we performed additional simulations of the action of TMAO on an intrinsically disordered Aβ_{16–22} (KLVFFAE) monomer. In the absence of TMAO, Aβ_{16–22} is a disordered random coil. However, in aqueous TMAO solution, Aβ_{16–22} monomer samples compact conformations. A transition from random coil to α-helical secondary structure is observed at high TMAO concentrations. The coil to α-helix transition is highly cooperative especially considering the small number of residues in Aβ_{16–22}. Our work highlights the potential similarities between the action of TMAO on long polypeptide chains and entropic stabilization of proteins in a crowded environment due to excluded volume interactions. In this sense, the chemical chaperone TMAO is a nanocrowding particle.



INTRODUCTION

Trimethylamine *N*-oxide (TMAO) is a naturally occurring osmolyte that accumulates in organisms to counteract the destabilizing effect of urea¹ on folded protein conformations. A number of experiments have shown that TMAO stabilizes proteins,^{2–4} but the precise molecular mechanism has not been firmly established.^{5–7} The stabilization of proteins by TMAO can be qualitatively understood from the perspective of an entropic stabilization mechanism introduced in the context of crowding effects on protein stability.⁸ Depletion of an osmolyte from the vicinity of proteins results in compact conformations, which stabilizes the native states.^{8–12} On the other hand, if an osmolyte were to interact directly with the protein, as is the case with denaturants such as urea and guanidinium hydrochloride, the native basin of the protein would be destabilized.^{13–15} These arguments, while rationalizing the different roles of protective and denaturing osmolytes, do not provide a molecular explanation of their actions.

The structure of TMAO (Figure 1) suggests that there are two main types of intermolecular interactions that are possible

between TMAO and proteins. The oxygen atom on TMAO (O_T) can act as a hydrogen bond acceptor. Three methyl groups in TMAO can participate in hydrophobic interactions with the side chains of proteins. From transfer free energy calculations, it has been deduced that TMAO has no significant preference for hydrophobic moieties, but TMAO interacts with the backbone, as well as charged and polar side chains.² It is necessary to extend such studies to systems in which chain connectivity and sequence effects are explicitly taken into account.

To dissect the molecular basis for the action of TMAO on peptides, we simulated five dipeptides in explicit water in 1 M TMAO. The dipeptides are ideal model systems for the study of TMAO–protein interactions because, like unfolded proteins, they are solvent exposed, and hence can freely interact with the surrounding solvent molecules. Each dipeptide was composed of one of the following types of amino acids: leucine (nonpolar),

Received: July 30, 2011

Revised: October 6, 2011

Published: October 10, 2011

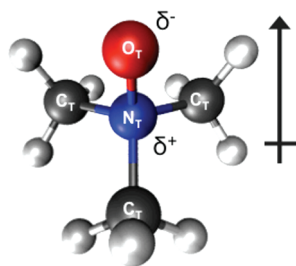


Figure 1. Structure of TMAO. The partial charges of the N-oxide group and the distribution of the dipole moment are identified. The values of partial charges, δ^+ and δ^- , are 0.44 and -0.65 , respectively.

serine (polar, hydroxyl group), glutamine (polar, amino group), and lysine (basic). In addition, we also studied conformational changes in diglycine (G_2) and hexaglycine (G_6), which has been recently investigated using MD simulations in aqueous TMAO solution.¹⁶ Comparison of the conformational changes in G_2 and G_6 in TMAO leads to the hypothesis that as the polypeptide chain length increases TMAO is expelled from the surface, which results in the collapse of the predominantly backbone construct. Consequently, G_6 adopts a conformation that maximizes the intrapeptide interactions. In order to further validate our hypothesis, we performed all-atom MD simulations of $A\beta_{16-22}$ (KLVFFAE) monomer, which aggregates to form amyloid fibrils, in various TMAO concentrations. The $A\beta_{16-22}$ peptide, which consists of a short sequence of hydrophobic residues flanked by two oppositely charged residues is disordered and adopts a random coil conformation that is devoid of secondary structure. Remarkably, $A\beta_{16-22}$ becomes helical upon interaction with increasing concentrations of TMAO. Analysis of the conformations of $A\beta_{16-22}$ shows that TMAO is depleted from the surface of the backbone, which establishes that TMAO-induced transition from random coil to α -helix is due the entropic stabilization mechanism. Thus, the stabilization of proteins by TMAO is akin to a mechanism by which crowding particles stabilize proteins, which suggests TMAO can be treated as a nanocrowding particle.

METHODS

We performed MD simulations using the NAMD program¹⁷ and the CHARMM22¹⁸ force field with the CMAP modification¹⁹ for proteins and waters. In order to describe the interactions between the osmolyte and the polypeptide chains, we used the TMAO force field parameters of Kast et al.²⁰ We first simulated five dipeptides and one hexaglycine in order to dissect the interaction between TMAO and polypeptide chains. Each dipeptide was composed of one of the following types of amino acids: leucine (nonpolar), serine (polar, hydroxyl group), glutamine (polar, amino group), and lysine (basic). The diglycine and hexaglycine molecules were simulated in the absence and presence of TMAO.

As a starting point, the fully extended peptide was centered in a rectangular water box comprised of TIP3P water molecules, and all of the water molecules within 2.2 Å of the peptide molecule were deleted. The dimension of the water box was set to 10 Å, which is more than the length of the peptide. We performed 10 independent simulations where the TMAO positions were set by randomly replacing the TIP3P water molecules such that the concentration was 1.0 M, a value that is typically used in transfer experiments. For each independent trajectory, 100 initial

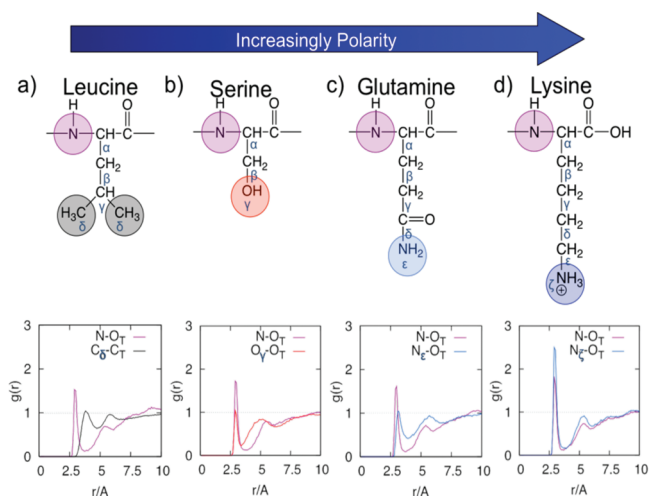


Figure 2. Radial distribution functions between atomic centers of TMAO and dipeptides: (a) leucine; (b) serine; (c) glutamine; (d) lysine. The amino acid chemical structures are at the top, and the corresponding radial distribution functions are below. The corresponding distribution of angles formed by hydrogen bonds formed by the peptide backbone amide N and H with the TMAO oxygen (O_T) are shown in Figure 3, and the pair functions involving other interaction sites are shown in Supporting Information Figure S1.

configurations with different placements of the TMAO were generated, followed by 10 steps of steepest-descent and 25 steps of adopted-basis Newton–Raphson minimization with harmonic constraints on the peptide, and only the lowest energy configuration was used for simulations. Therefore, each independent simulation started from a unique, energy-minimized, random distribution of TMAO. We equilibrated the system by removing all harmonic constraints, applying 2000 steps of conjugate gradient minimization, and performing 50 ps of NVT MD simulations using a 2 fs time step. We then performed 10 ns production runs for NPT simulations of each di- and hexa-peptide at 298 K using the CHARMM force field. All analyses were performed for each production run.

For the $A\beta_{16-22}$ (KLVFFAE) monomer peptide simulations, the same protocol was used as with the di- and hexa-peptides except that the dimensions of the water box were cubic with each side of length 40 Å. The equilibration time period was increased to 5 ns, and the production run time length was increased to 100 ns at 300 K, of which the last 60 ns was used for analyses. Four sets of $A\beta_{16-22}$ monomer simulations were performed at TMAO concentrations of 0, 1.0, 2.5, and 5.0 M.

RESULTS AND DISCUSSION

TMAO Preferentially Interacts with the Peptide Backbone and Basic Dipeptide Side Chains. For the simulations of the leucine dipeptide (Figure 2a), the radial distribution function, $g(r)$, between O_T and the peptide backbone nitrogen (N), which is the only hydrogen bond donor, resulted in a peak with $g(r \approx 3 \text{ Å}) \sim 1.5$. At the typical hydrogen bond distance, $r \approx 3 \text{ Å}$, the most probable value of the angle between N, the amide hydrogen, and O_T is 150° (Figure 3a). The $g(r)$ between the TMAO methyl carbon (C_T) and the carbon atom of the terminal methyl group in the leucine side chain has a modest peak where $g(r) \sim 1.0$ at, $r \approx 4 \text{ Å}$, which shows that the dispersion interactions with the side chain are negligible (Figure 2a). Since leucine is the most

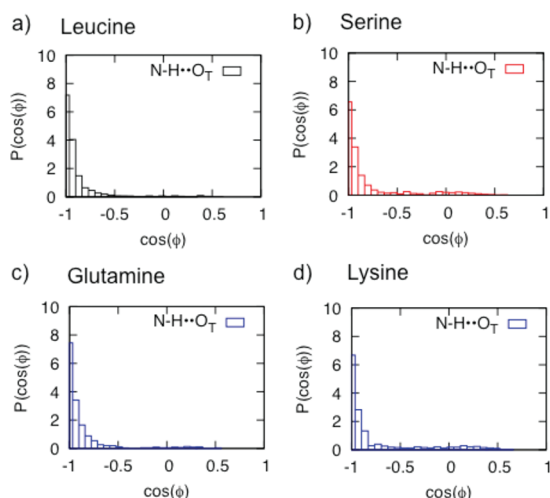


Figure 3. Distribution of angles formed by hydrogen bonds between the peptide backbone amide N and H with the TMAO oxygen (O_T) for the dipeptide constructs of (a) leucine, (b) serine, (c) glutamine, (d) lysine, and (e) glycine, as well as the hexaglycine construct. The angles exceeding 150° , which are characteristic of a perfect hydrogen bond, are most probable. Only interactions for which the distance between the backbone amide and TMAO is less than 3.5 \AA , which corresponds to the first solvation shell, are considered. Thus, at the distance when $g(r)$ has a first peak in all dipeptides, O_T forms a hydrogen bond with the amide proton. See Supporting Information Figure S2 for the corresponding hydrogen bond distribution of angles for the dipeptide and hexapeptide constructs of glycine.

hydrophobic residue, the interaction between TMAO and any other hydrophobic side chain must be less favorable in comparison to hydrogen bonding with the backbone. Serine and glutamine dipeptides (Figure 2b,c), which have hydroxyl and amino hydrogen bond donors, respectively, in the side chains, also resulted in $g(r) \sim 1.5$ for the backbone nitrogen but $g(r) \sim 1.0$ for the side chain oxygen (O_γ in serine) and nitrogen atoms (N_ϵ in glutamine). Interestingly, there is a greater preference for TMAO to hydrogen bond with the backbone nitrogen than the side chain hydrogen bond donors, including the amino nitrogen of glutamine (Figure 3b,c).

The $g(r \approx 3 \text{ \AA}) \sim 1.5$ peak is independent of the polarity of the side chains (Figure 2). In lysine dipeptide, however, there is also a pronounced peak ($g(r \approx 3 \text{ \AA}) \sim 2.5$) between O_T and the charged side chain amino nitrogen (N_ϵ) without compromising the hydrogen bond formation with amide nitrogen (Figures 2d and 3d). Clearly, it is possible for charged side chain hydrogen bond donors to have significant interactions with TMAO. We expect similar results for TMAO interactions with other basic amino acids, but their relative abundance in proteins suggests that the overall significance of TMAO–side chain interactions may not be significant. Interestingly, the radial distribution functions in Figure 2 also show that the size of the side chain does not affect the extent of interactions with the backbone nitrogen atom, as long as the backbone is solvent-exposed.

The preferential interaction of TMAO with the backbone hydrogen bond donor over the uncharged side chain hydrogen bond donor can be understood in structural terms. The peptide backbone forms a resonance interaction between the nitrogen atom and the carbonyl group. Thus, the peptide bond not only has a partial double bond character, it also leaves the nitrogen with a partial positive charge (and the carbonyl oxygen with a

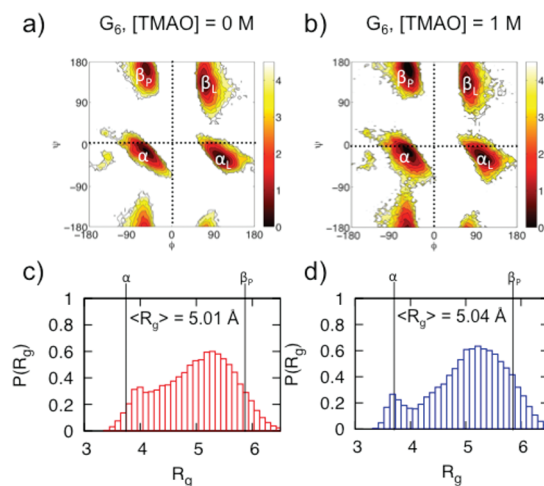


Figure 4. Conformations adopted by hexaglycine in the absence (a, c) and presence of 1 M TMAO (b, d). The Ramachandran free energy profiles are shown with the four major basins labeled (a, b). The normalized histograms of the radius of gyration, R_g , are shown with the R_g of ideal α -helices and PPII β -sheets labeled.

partial negative charge).²² Therefore, TMAO would form more favorable hydrogen bond interactions with the partially charged backbone nitrogen than an uncharged side chain hydrogen bond acceptor and an even greater favorable interaction with fully charged side chain amino nitrogen, as explicitly shown for lysine. Of course, asparagine and glutamine side chain amides can also participate in resonance stabilization such that the amide nitrogen has a partial charge but the electronegativity of its neighbors makes its overall partial charge less than that of the peptide amide nitrogen.

TMAO—Peptide Group Interactions Depend on the Length of the Polypeptide. The dipeptides are not long enough to form intramolecular interactions. Thus, it is not possible to investigate the propensity to form TMAO-induced secondary structure formation. A recent paper²¹ found that in the absence of TMAO the backbone hydrogen bonds are primarily responsible for the collapse of the peptide chains. It follows that if the solvent and TMAO are depleted from the vicinity of the polypeptide chain, then it can collapse by maximizing the number of intramolecular hydrogen bonds. To assess if such a mechanism is operative, we monitored osmolyte-induced changes in the collapse and secondary structural elements, and the dependence of polypeptide length on TMAO interactions we simulated hexaglycine (G_6) for which the conformational space can be fully explored on a nanosecond time scale. Although G_6 is unlikely to form a well-ordered secondary structure because the enthalpically favorable hydrogen bonds cannot overcome the entropy loss, TMAO can alter the population of the most probable (ϕ, ψ) angles that are adopted in water. The polyglycine chain is also an excellent model system for the study of backbone dynamics in pure water and in TMAO solutions due to the absence of side chain moieties.¹⁶ The backbone dihedral angles of G_6 populate four sets of conformations that correspond to the left- and right-handed α -helices and PPII β -sheet-like conformations in water (Figure 4a). The addition of 1 M TMAO shifts the Ramachandran folding free energy profiles by expanding the region corresponding to the α -helical basin (Figure 4b). The distribution of the radius of gyration (R_g) over all ten 10 ns trajectories shows a clear increase in the relative population of structures with R_g close to

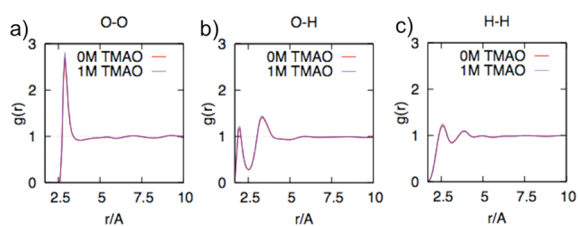


Figure 5. Comparison of the radial distribution functions involving water interaction sites in pure water (0 M) and 1 M TMAO solution for hexaglycine simulations. The interwater O–O, O–H, and H–H radial distribution functions, $g(r)$, are shown. The structure of water is not significantly perturbed in TMAO solution containing G_6 .

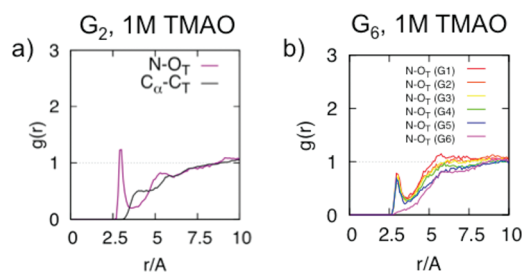


Figure 6. Pair functions between TMAO and (a) diglycine and (b) hexaglycine.

that of an ideal α -helical G_6 (Figure 4c,d). Interestingly, $\langle R_g \rangle$ is similar to the value obtained by Shortle and co-workers from their NMR and SAXS measurements, which show a value intermediate between ideal α -helices and PPII β -sheets.²³

The radial distribution functions involving the atomic interactions of water are almost quantitatively identical in pure water and 1 M TMAO (see Figure 5), even in the presence of hexaglycine. These results show that the structural changes observed in G_6 have to be related to the depletion of TMAO with the polypeptide chain. Since α -helical G_6 conformations can have up to two intramolecular hydrogen bonds of the backbone nitrogen (with the backbone carbonyl oxygen that is separated by four amino acids earlier in sequence), we calculated the $g(r)$ between the N and O_T . The $g(r)$ value for G_6 is much lower than that for diglycine (G_2) (Figure 6a,b), which we use as a control because it is too short to form intramolecular hydrogen bonds. The enhancement of the α -helical basin in 1 M TMAO in G_6 is due to its depletion from around the peptide backbone, which is in accord with previous studies.² Thus, the formation of α -helical structure disfavors backbone hydrogen bond formation with TMAO, but the backbone amide nitrogen still favors hydrogen bonding with the carbonyl oxygen because of its larger dipole moment and proximity as compared to the TMAO oxygen. The differences in $g(r)$ between N and O_T in G_2 and G_6 highlight the role of chain length in TMAO–peptide interaction. For G_2 , the amide nitrogen is accessible to O_T , which is consistent with simulations of cyclic G_2 .⁵

TMAO is a Nano-Crowding Agent. Observations of ordered secondary structure in 1 M TMAO in G_6 can be rationalized using the depletion theory used to predict stability changes in the folded states in a crowded environment. Depletion of TMAO around G_6 essentially induces an osmotic pressure²⁴ on G_6 , which results in chain compaction, as was previously observed in MD simulations of the longer G_{15} in TMAO.²⁵ Thus, the polypeptide

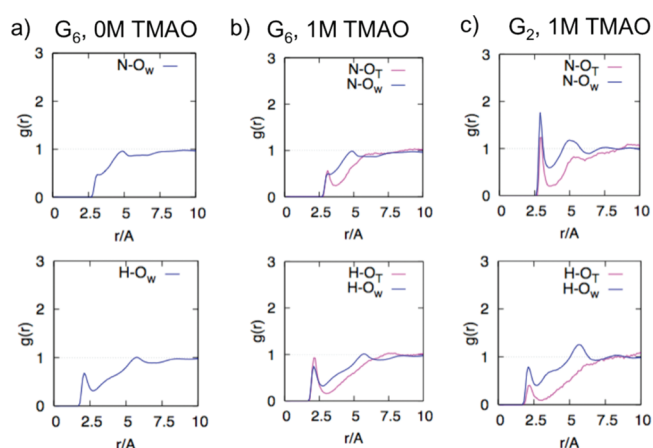


Figure 7. Pair functions between various amide backbone atoms from (a,b) hexaglycine and (c) diglycine constructs and atomic centers on water and TMAO. The top row consists of radial distribution functions, $g(r)$, between the backbone amide nitrogen (N) and the oxygens of water (O_w) and TMAO (O_T). The bottom row is the same except with backbone amide hydrogen (H). In the presence of TMAO, the strength of the hydrogen bond involving the amide N is suppressed. The decrease is dramatic when the results for G_2 and G_6 are compared. Interestingly, the amide N in G_6 does not even form hydrogen bonds with O_w when TMAO is present. Thus, both the solvent and the solute (TMAO) are depleted from the surface of G_6 . This effect is essentially similar to the entropic stabilization in the excluded volume dominated crowding agents.

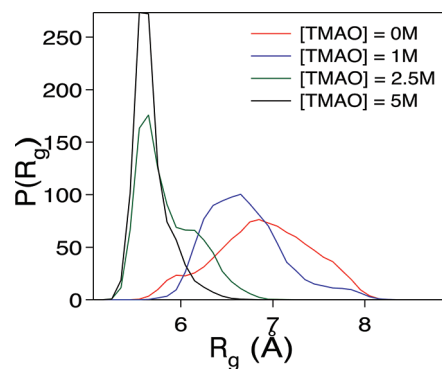


Figure 8. Probability distribution of R_g of $A\beta_{16-22}$ in various TMAO concentrations.

is forced to adopt conformations that maximize intramolecular interactions. In the G_6 case, this results in an increase in the population of α -helical structure (Figure 4b). The exclusion of TMAO from G_6 is vividly illustrated using a number of pair functions involving water, TMAO, and the amide nitrogen (Figure 7a,b). Thus, in 1 M TMAO, G_6 is localized in a region that is devoid of both water and TMAO. Such a mechanism is exactly the one invoked to quantitatively predict the native state stabilization in a crowded environment due to volume excluded to the protein by the crowding particles!

Two remarks of caution are in order. (1) For small peptides such as G_2 , the amide nitrogen interacts favorably with O_w and O_T (Figure 7c). Thus, polypeptide chain length is important in observing TMAO-induced structure formation. (2) More importantly, it is known from crowding theory^{11,12} that the nature of the structures adopted depends on $q = \langle R_g \rangle / R_c$, where R_c is the size of the crowding particles. In our study of G_6 in TMAO,

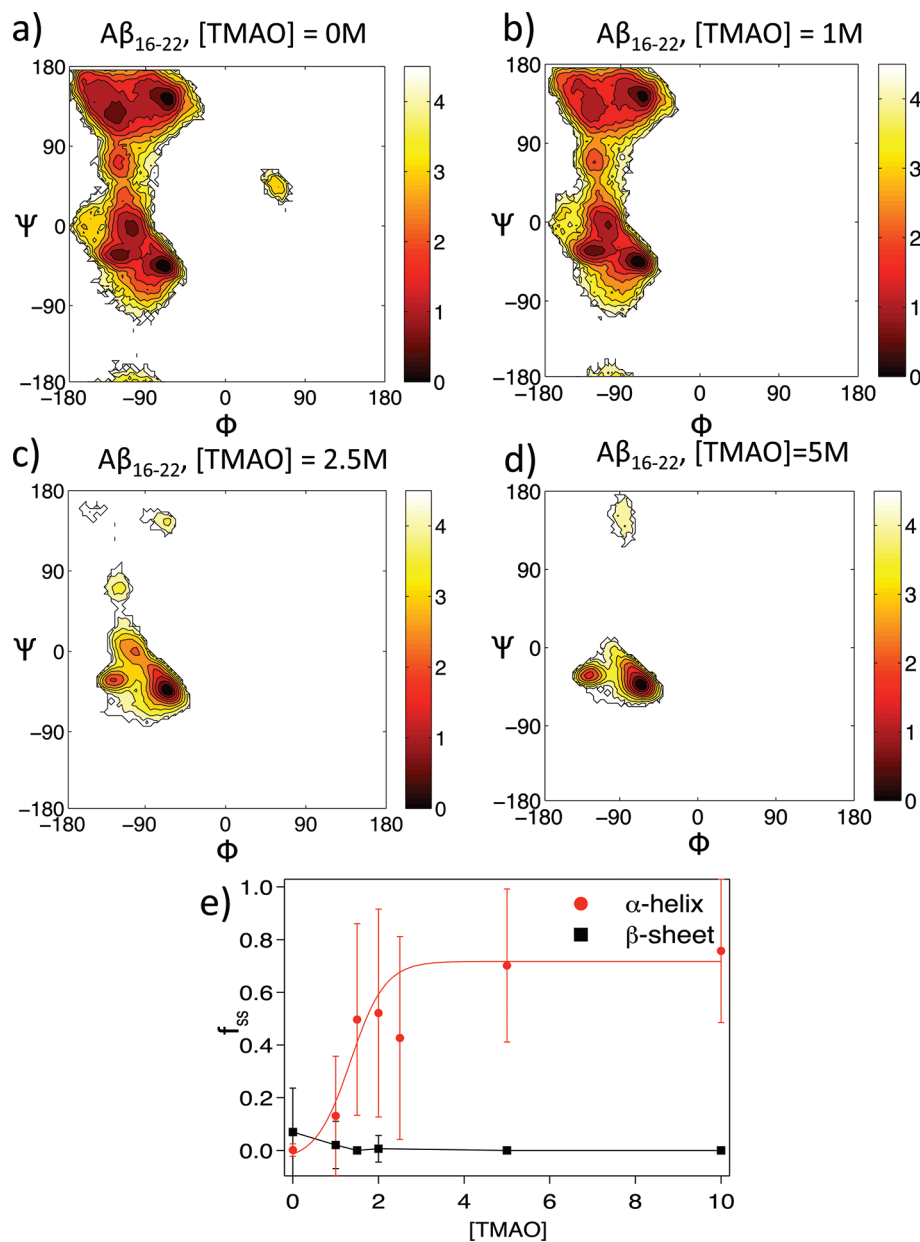


Figure 9. Ramachandran free energy profiles of $A\beta_{16-22}$ at TMAO concentrations of (a) 0 M, (b) 1 M, (c) 2.5 M, and (d) 5 M. The cooperative transition from random coil to α -helix transition is shown in part e. This panel also shows that at all TMAO concentrations there is negligible β -strand content.

$\langle R_g \rangle = 5.01 \text{ \AA}$ and $R_c = 1.32 \text{ \AA}$, resulting in $q \approx 3.77$. It is unclear whether depletion theory also holds if q and sequence are varied.

$A\beta_{16-22}$ Peptide Becomes Compact and α -Helical with Increasing TMAO Concentration. In order to assess if the depletion mechanism leading to a shift in the population toward α -helical structure is general, we used simulations to probe TMAO-induced changes in $A\beta_{16-22}$ (KLVFFAE) monomer peptide, which aggregates to form antiparallel fibrils²¹ at high peptide concentration. We had shown earlier that $A\beta_{16-22}$ monomer is a random coil largely devoid of secondary structure. In particular, the population of α -helical structure is less than about 1%. If TMAO acts as a nanocrowder, then we expect that $A\beta_{16-22}$ would be localized in a region devoid of TMAO. Under these conditions, $A\beta_{16-22}$ is expected to adopt an α -helical conformation to maximize intramolecular interactions.²⁶ In order

to test the applicability of depletion-induced structure formation, we performed simulations of $A\beta_{16-22}$ in various TMAO concentrations.

In addition to being a biologically relevant system, the intrinsically disordered $A\beta_{16-22}$ peptide is a very good model system to study the role of TMAO on conformational fluctuations of peptides, since its sequence consists of charged residues, a positive lysine (K), and a negative glutamic acid (E), that cap the ends of a short stretch of hydrophobic residues. The probability distribution of the radius of gyration, $P(R_g)$, of the $A\beta_{16-22}$ peptide shows that it becomes more compact with increasing TMAO concentration (Figure 8). The values of mean R_g , $\langle R_g \rangle$ ($= \int P(R_g) dR_g$) for the TMAO concentrations, [TMAO] = 0, 1.0, 2.5, and 5 M, are 6.9, 6.7, 5.9, and 5.7 \AA , respectively. Thus, there is a 17% reduction in $\langle R_g \rangle$ as [TMAO] is changed from 0 to 5 M.

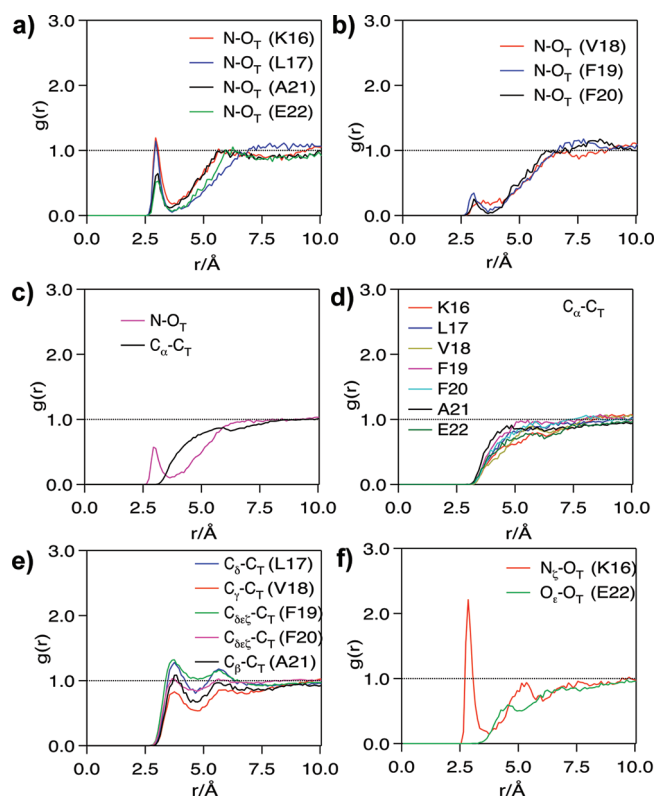


Figure 10. Radial distribution functions between atomic centers of TMAO and $A\beta_{16-22}$. (a) The TMAO oxygen (O_T) interactions with the backbone amide N of the termini residues of the $A\beta_{16-22}$ peptide. (b) The O_T interactions with backbone amide N of residues in the interior of the $A\beta_{16-22}$ peptide. The only significant TMAO interactions with the backbone amide N are observed for those in the N-terminal residues. (c) A comparison of the total backbone polar amide N with O_T vs hydrophobic C_α interactions with the TMAO carbon C_T , as well as (d) the individual per residue hydrophobic C_α interactions. There are no significant hydrophobic backbone C_α interactions with TMAO. (e) Hydrophobic side chain interactions with C_T show that these interactions can be modestly significant. (f) The polar side chain interactions with O_T show a clear and significant preference of TMAO for the positively charged lysine side chain.

We further probed the structural changes by calculating the Ramachandran free energy profiles of the peptide. In the absence of TMAO, $A\beta_{16-22}$ fluctuates among a number of distinct structures. Figure 9a,b shows that for $A\beta_{16-22}$ the basins with (ϕ, ψ) angles that correspond to β -sheets and α -helices are populated, as would be expected from an intrinsically disordered peptide that is basically a random coil. In the absence of TMAO, $A\beta_{16-22}$ has negligible α -helical or β -strand content (Figure 9e), which accords well with our earlier study.²⁶ At a modest concentration of TMAO (i.e., $[TMAO] = 2.5$ M), the β -strand basins disappear (Figure 9c). Remarkably, for $[TMAO]$ greater than 2.5 M, only the right-handed α -helices remain (Figure 9c,d). Thus, TMAO induces a transition between a predominantly random coil state to α -helical structure. Considering the small size of $A\beta_{16-22}$, the transition is relatively sharp, as assessed by the cooperativity measure.²⁷ Similar results are experimentally observed where TMAO induces helical formation in alanine peptides.²⁸

The tendency of $A\beta_{16-22}$ to form ordered α -helical structures has implications for oligomer formation. The formation of stable helical structure could preclude amyloid formation, which requires β -structures as seeds. It is interesting to contrast

TMAO-induced structure formation to the effects of urea on $A\beta_{16-22}$. Molecular dynamics simulations showed that in urea $A\beta_{16-22}$ monomer is extended and forms β -strands.²⁹ The contrasting behavior could have implications for aggregation in mixed cosolvents containing urea and TMAO.

TMAO Interacts with the $A\beta_{16-22}$ Backbone and Lysine Side Chain. To determine the molecular interactions that induce the helical formation of the $A\beta_{16-22}$ (KLVFFAE) peptide, we calculated the radial distribution function, $g(r)$, between TMAO and the $A\beta_{16-22}$ peptide. There is a stronger preference for terminal (K16, L17, A21, and E22) backbone amide N with TMAO (Figure 10a) compared with those in the interior (V18, F19, and F20) (Figure 10b), which may be a reflection of the bulky phenylalanine that effectively excludes interactions with the peptide backbone. The TMAO interactions with the backbones of these residues are more pronounced for polar interactions with the amide N (Figure 10c,d). The residence time of TMAO near the backbone atoms is approximately 55 ps, which is approximately twice that of water. The residence time is defined as the time during which any of the TMAO or water atoms are within 4 Å of any of the backbone atoms. Hydrophobic interactions with TMAO are modestly significant for the side chains (Figure 10e) and nonexistent in our simulations for the backbone (Figure 10d). The interactions between TMAO and the terminal positively charged lysine side chain, however, are pronounced (Figure 10f), even more than interactions with the terminal backbone amide N (Figure 10a). The affinity of TMAO to negatively charged side chains is minimal (Figure 10f).

CONCLUSIONS

Using all-atom MD simulations of a number of model peptide constructs and $A\beta_{16-22}$ monomer in aqueous TMAO solution, we dissected the molecular mechanism of how TMAO stabilizes the native basin of proteins. By preferentially hydrogen bonding to the backbone nitrogen of the solvent exposed peptides, TMAO acts as a nano “crowder” that limits the degrees of freedom of the unfolded state and entropically destabilizes it. When the backbone nitrogen forms a secondary structure, it is no longer available to hydrogen bond with TMAO, resulting in the depletion from the vicinity of the protein, which in turn results in native state stabilization. Comparisons between G_2 and G_6 show that polypeptide length is a relevant factor in determining the energetic balance between collapsed and extended structures. If the polypeptide chain exceeds a critical size, it is likely that aqueous TMAO would be a “poor” solvent for generic proteins, which would promote collapse and structure formation, as demonstrated for $A\beta_{16-22}$ peptide. In particular, TMAO induces a highly cooperative coil to α -helix transition, a prediction that can be easily tested. Finally, our work also shows that in sequences that contain charged residues (e.g., intrinsically disordered proteins or fragments of $A\beta$ peptides, such as $A\beta_{16-22}$), the interactions between TMAO and positively charged side chains are significant. However, for generic proteins, TMAO is expelled from the surface. In this sense, TMAO behaves as a nanocrowding particle, thus stabilizing proteins by the entropic stabilization mechanism.¹⁰

ASSOCIATED CONTENT

S Supporting Information. Radial distribution functions between amide N and H in dipeptide constructs and oxygens of water and TMAO. Pair functions between amide N and H in

glycine constructs and oxygens of water and TMAO. Distribution of hydrogen bond angles formed between dipeptide and hexapeptide constructs of glycine and TMAO. This material is available free of charge via the Internet at <http://pubs.acs.org>.

AUTHOR INFORMATION

Corresponding Author

*E-mail: thirum@umd.edu.

Present Addresses

[†]Departments of Physics and Computer Science, Wake Forest University, Winston-Salem, North Carolina, 27109.

ACKNOWLEDGMENT

This work was supported in part by a grant from the National Science Foundation (CHE 09-10433). S.S.C. was supported by a Ruth L. Kirschstein National Research Service Award from the National Institutes of Health.

REFERENCES

- (1) Yancey, P. H.; Clark, M. E.; Hand, S. C.; Bowlus, R. D.; Somero, G. N. *Science* **1982**, *217*, 1214–1222.
- (2) Wang, A.; Bolen, D. W. *Biochemistry* **1997**, *36*, 9101–9108.
- (3) Baskakov, I.; Bolen, D. W. *J. Biol. Chem.* **1998**, *273*, 4831–4834.
- (4) Auton, M.; Bolen, D. W. *Proc. Natl. Acad. Sci. U.S.A.* **2005**, *102*, 15065–15068.
- (5) Zou, Q.; Bennion, B. J.; Daggett, V.; Murphy, K. P. *J. Am. Chem. Soc.* **2002**, *124*, 1192–1202.
- (6) Street, T. O.; Bolen, D. W.; Rose, G. D. *Proc. Natl. Acad. Sci. U.S.A.* **2006**, *103*, 13997–14002.
- (7) Paul, S.; Patey, G. N. *J. Phys. Chem. B* **2007**, *111*, 7932–7933.
- (8) Minton, A. P. *Curr. Opin. Struct. Biol.* **2000**, *10*, 34–39.
- (9) Minton, A. P. *Biophys. J.* **2005**, *88*, 971–985.
- (10) Cheung, M. S.; Klimov, D.; Thirumalai, D. *Proc. Natl. Acad. Sci. U.S.A.* **2005**, *102*, 4753–4758.
- (11) Shaw, M. R.; Thirumalai, D. *Phys. Rev. A* **1991**, *44*, R4797–R4800.
- (12) Pincus, D. L.; Hyeon, C.; Thirumalai, D. *J. Am. Chem. Soc.* **2008**, *130*, 7364–7372.
- (13) Robinson, D. R.; Jencks, W. P. *J. Am. Chem. Soc.* **1965**, *87*, 2462–2470.
- (14) O'Brien, E. P.; Dima, R. I.; Brooks, B.; Thirumalai, D. *J. Am. Chem. Soc.* **2007**, *129*, 7346–7353.
- (15) Auton, M.; Holthausen, L. M.; Bolen, D. W. *Proc. Natl. Acad. Sci. U.S.A.* **2007**, *104*, 15317–15322.
- (16) Hu, C. Y.; Lynch, G. C.; Kokubo, H.; Pettitt, B. M. *Proteins: Struct., Funct., Bioinf.* **2010**, *78*, 695–704.
- (17) Phillips, J. C.; Braun, R.; Wang, W.; Gumbart, J.; Tajkhorshid, E.; Villa, E.; Chipot, C.; Skeel, R. D.; Kale, L.; Schulten, K. *J. Comput. Chem.* **2005**, *26*, 1781–1802.
- (18) MacKerell, A. D.; Bashford, D.; Bellott, M.; Dunbrack, R. L.; Evanseck, J. D.; Field, M. J.; Fischer, S.; Gao, J.; Guo, H.; Ha, S.; Joseph-McCarthy, D.; Kuchnir, L.; Kuczera, K.; Lau, F. T. K.; Mattos, C.; Michnick, S.; Ngo, T.; Nguyen, D. T.; Prodhom, B.; Reiher, W. E.; Roux, B.; Schlenkrich, M.; Smith, J. C.; Stote, R.; Straub, J.; Watanabe, M.; Wiorkiewicz-Kuczera, J.; Yin, D.; Karplus, M. *J. Phys. Chem. B* **1998**, *102*, 3586–3616.
- (19) MacKerell, A. D.; Feig, M.; Brooks, C. L. *J. Am. Chem. Soc.* **2004**, *126*, 698–699.
- (20) Kast, K. M.; Brickmann, J.; Kast, S. M.; Berry, R. S. *J. Phys. Chem. A* **2003**, *107*, 5342–5351.
- (21) Teufel, D. P.; Johnson, C. M.; Lum, J. K.; Neuweiler, H. *J. Mol. Biol.* **2011**, *409*, 250–262.

(22) Pauling, L. *The nature of the chemical bond and the structure of molecules and crystals; an introduction to modern structural chemistry*, 3rd ed.; Cornell University Press: Ithaca, NY, 1939.

(23) Ohnishi, S.; Kamikubo, H.; Onitsuka, M.; Kataoka, M.; Shortle, D. *J. Am. Chem. Soc.* **2006**, *128*, 16338–16344.

(24) Oosawa, F.; Asakura, S. *J. Chem. Phys.* **1954**, *22*, 1255–1255.

(25) Hu, C. Y.; Lynch, G. C.; Kokubo, H.; Pettitt, B. M. *Proteins: Struct., Funct., Bioinf.* **2010**, *78*, 695–704.

(26) Klimov, D. K.; Thirumalai, D. *Structure* **2003**, *11*, 295–307.

(27) Klimov, D. K.; Thirumalai, D. *Folding Des.* **1998**, *3*, 127–139.

(28) Celinski, S. A.; Scholtz, J. M. *Protein Sci.* **2002**, *11*, 2048–2051.

(29) Klimov, D. K.; Straub, J. E.; Thirumalai, D. *Proc. Natl. Acad. Sci. U.S.A.* **2004**, *101*, 14760–14765.